EXTERNAL AND INTERNAL ELECTROMAGNETIC EXPOSURES OF WORKERS NEAR HIGH VOLTAGE POWER LINES

N. M. Maalej and C. A. Belhadj

King Fahd University of Petroleum and Minerals
Dhahran, Saudi Arabia

Abstract—The major objective of the study was to assess the safety of electric line workers exposed to of a double circuit 132 kV transmission line for different scenarios. The double circuit 132-kV, 60 Hz transmission line has a power rating of 293 MVA and a maximum recorded peak load current of 603 A. The charge simulation and the Biot Savart methods were used by EPRI workstation software to compute the external electric and magnetic fields around a 132 kV transmission line. We used the calculated external electric and magnetic field exposures to determine the induced electric field and induced current densities inside the human body. This was performed using the Finite Difference Time Difference computational algorithm in EMPIRE commercial software, with a 6 mm voxel resolution. We used the Visible Human (VH) to investigate the internal induced electric field and circulating current densities in more than 40 different tissues and organs of the VH. We found that the worker exposure levels to extremely low frequency electromagnetic fields are below the recommended IEEE international standards limits for the studied scenarios. In all scenarios the maximum induced current densities and electric fields were in the bone marrow of the feet.

1. INTRODUCTION

There is a growing concern among electric utilities workers regarding possible health hazards due to the exposure to power frequency electromagnetic fields. The aim of this project was to assess and evaluate the safety of the electric line workers who are exposed to Extremely Low Frequency-Electromagnetic Field (ELF-EMF) that are produced by High Voltage (60 Hz) transmission lines.

There has been a growing interest over the years in determining the safe exposure levels of people, mainly workers, and the general public, to power frequency electric and magnetic fields. Several organizations have developed standards and guidelines for such permissible exposure levels. By far, the most important organizations that have contributed to the establishment of these standards and guidelines are the Institute of Electrical and Electronics Engineers (IEEE) [1], and the International Commission on Non-Ionizing Radiation Protection (ICNIRP) [2]. There are other organizations such as the American Conference of Governmental Industrial Hygienists (ACGIH) and The National Radiological Protection Board (NRPB) in the UK [3]. The permissible levels quoted in many countries refer to the permissible levels set by the IEEE standard or the ICNIRP guideline. Table 1, columns 3 to 5, show the list of external exposure limits for 60 Hz for the IEEE, ICNIRP and NRPB. Table 2 lists a summary of internal exposure limits for the same frequency.

In this study, we investigate both the external electric and magnetic fields and the internal electric fields and current densities induced in the human body tissues and organs of a live-line worker standing 2 m away from phase A, B and C conductors, under the tower, under the mid-span and at the edge of the right-of-way of a double circuit 132 kV transmission line. The results are compared with the IEEE and ICNIRP exposure limits to verify compliance and the safety from the possible short term effects to extremely high voltages at power frequency.

In recent years, a number of laboratories have developed heterogeneous models of the human body with an anatomical shape and numerous tissues to study the electromagnetic field (EMF)

Table 1. Summery of external exposure limit of electric and magnetic fields from different regulating organizations at 60 Hz frequency.

Organization		Occupational	General Public
IEEE	Electric Field	20 kV/m	5 kV/m
	Magnetic Field	2.71 mT (Head & Torso)	0.904 mT (Head & Torso)
ICNIRP	Electric Field	8.33 kV/m	4.17 kV/m
	Magnetic Field	1 mT	0.2 mT
NRPB	Electric Field	12 kV/m	12 kV/m
	Magnetic Field	1.6 mT	1.6 mT
ACGIH	Electric Field	25 kV/m	
	Magnetic Field	1 mT	

Table 2. Summery of internal exposure limits from different regulating organizations at 60 Hz frequency.

Organization	Organ	Occupational	General Public
IEEE	Brain	53.1 mV/m	17.7 mV/m
	Heart	943 mV/m	943 mV/m
	Hands, wrists, feet and ankles	2100 mV/m	2100 mV/m
	Other tissue	2100 mV/m	701 mV/m
ICNIRP	Central Nervous System (CNS) tissues of head	120 mV/m	24 mV/m
	All other tissues	800 mV/m	400 mV/m
NRPB	Central Nervous System (CNS)	10 mA/m^2	10 mA/m^2

exposure. Most of these models have been developed by computer segmentation of data from magnetic resonance imaging (MRI) [4–7]. These groups and others have used the high resolution human body models to study the EMF exposures of the human body to low and high frequencies.

The high resolution models and advanced numerical methods have been used to calculate the EMF exposure at high frequencies [7–9]. Recently, Kuhn et al. investigated RF exposure and absorption characteristics for various anatomies ranging from 6 years old child to large adult male by numerical modeling [10]. Hand reviewed the different calculation method and anatomical models for high frequency electromagnetic exposure [11].

Several methods have also been developed to study electric fields and current densities induced in anatomic models of the human body for low frequency exposure [12, 16]. Gandhi used the quasi-static impedance method to calculate the currents induced in the nominal $2 \times 2 \times 3$ and 6 mm resolution anatomically based models of the human body for exposure to magnetic fields at 60 Hz from homogeneous and non-homogeneous magnetic fields [14]. Dawson and Stuchly used the scalar potential finite difference (SPFD) method approach that resulted in a high computational efficiency for 3.6 mm voxel model [12]. Dimbylow used both the impedance method and the scalar potential finite difference methods in a fine-resolution (2 mm) anatomically realistic voxel model [16].

In this work, we determine the external electric and magnetic field intensities from a 132 kV power line at different positions (scenarios) in the vicinity of the transmission line using EPRI workstation software.

These external field values are used in Empire software to investigate the induced electric fields and current densities inside the human body of a live-line worker in these scenarios. The results are compared with the IEEE and ICNIRP exposure limits to verify compliance with the safety requirements of power-line workers.

2. METHODS

2.1. Exposure Scenarios and External Exposure Calculation

A typical double circuit transmission line was selected by Saudi Electric Company (SEC). The nominal voltage and power ratings are 132 kV and 293 MVA respectively. The study was conducted for 6 different exposure scenarios. These scenarios are illustrated in Figure 1. These scenarios cover the most probable locations of a live line worker near a transmission line. The worker body was assumed to be standing in free space and not in contact with electrical ground.
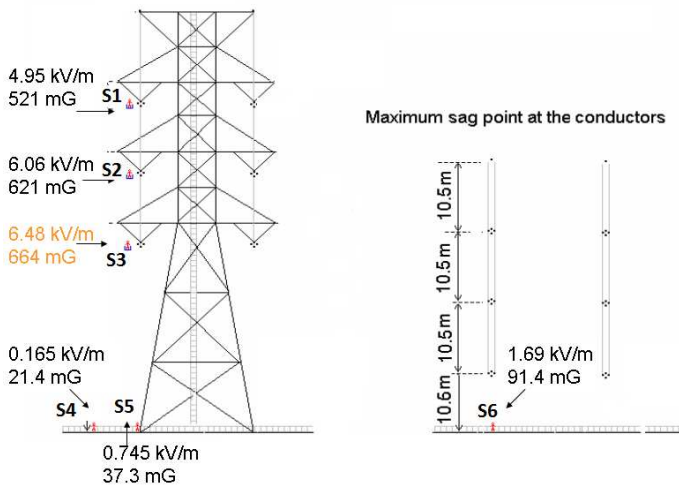
Figure 1. Simulated Scenarios **(S1-S6)** with corresponding maximum external electric and magnetic fields; **S1**: a worker standing 2 m away and facing the phase A conductor of a double circuit 132 kV power line; **S2**: a worker standing 2 m away and facing the phase B conductor; **S3** a worker standing 2 m away and facing phase C conductor; **S4**: A worker standing on the ground at the edge of the right-of-way of the transmission line; **S5**: A worker standing on the ground at the edge of the tower; **S6**: A worker standing on the ground below the transmission line under the mid-span (maximum sag point).

Quantitative description of the electrostatic field around overhead transmission lines has been presented in many references [17–26]. We have used the charge simulation method (CSM) that applies for domains with open boundaries and has no restriction with regards to the geometry of the domain [23, 27]. We particularly used EMF WORKSTATION Package developed by Electric Power Research Institute (EPRI) to calculate the electric field levels [27]. CSM accuracy has been verified analytically in the user's manual, Version 2.5.1 of the EMF WORKSTATION [27] and by measurement by Deno and Zaffanella [28]. The software package used, starts by setting the general required parameters such as the designated area of concern parameters, the structure position, boundary area, as well as the field calculation height. The line design parameters are entered in a detailed manner and include the phase structure of the line, the conductor size, the applied voltage and the operating current. The span specifications are also taken in consideration.

2.2. Internal Exposure Calculation

We have adopted the Finite Difference Time Domain (FDTD) method to solve Maxwell's equations to calculate the internal fields. The FDTD was first introduced by Yee in 1966 as a numerical technique to solve the Maxwell's equation for electromagnetic fields interaction with materials [29]. This method is based on the discretization of the Maxwell's equations, and involves sampling the electric and magnetic fields distributions in space and in time. The simulation results were validated by comparing the results with the analytical solutions for simple geometries. Our results for the human body internal exposures were also validated with previously published data [30].

We used EMPIRE software (IMST, Germany) in order to obtain the induced current densities and electric field inside the human body caused by exposures to external power line electric and magnetic fields. EMPIRE software uses the FDTD method to solve Maxwell's equations. At low frequency (60 Hz) the program makes use of the quasi-static formulation to evaluate the induced electric fields and currents in the human body from the exposure to external electric and magnetic fields. Due to the quasi-static situation of low frequency, exposure to the two fields, electric and magnetic, can be computed separately and the induced fields are added at the end of the simulations.

2.3. Visible Human Heterogeneous Model

EMPIRE software uses the anatomical human body from the visible human project (National Library of Medicine) [31]. The body model is obtained from Computerized Tomography (CT) and Magnetic Resonance Imaging (MRI) images of a male body. The male body was cryosectioned. The heterogeneous model has more than 40 different tissues. The model is available with 1, 2 and 3 mm voxel sizes. Each voxel is specified by its location in three-dimensional space and by its tissue type. We used the 6 mm voxel size to determine the induced EMF exposures for a person standing under the power line [32]. We also used the 3 mm voxel size for the worker standing 2 meters away from phase C conductor [33]. Running the simulation for the 3 mm resolution is very time consuming and requires much more computer memory and time compared to the 6 mm model. In this study, we used the 6 mm voxel size to determine the internal exposure parameters for commonly encountered scenarios for the power line workers. The 6 mm computation mesh in FTDT will consider the voxel tissue to be that of the most prevalent tissue covered by the volume of the voxel. Hence, the small size tissues such as the CSF will be shadowed by the surrounding dominant tissues. However, for large tissues and organs the difference between the results for the 3 and 6 mm voxels is not very significant [34].

For this heterogeneous body model, we used the tissue electrical properties of conductivity (σ), permittivity (ε), and the permeability (μ) published by Gabriel et al. [35]. At low frequencies ($< 100\,\mathrm{Hz}$) the induced conduction current (related to conductivity) is 2 to 4 orders of magnitude higher than the displacement current (related to permittivity). Thus, it is sufficient to consider the conductivity and neglect the permittivity of the tissue during computation [4, 5].

In order to calculate the induced electric fields and current densities inside the human body for each scenario, an input file has been prepared for the simulation. The input file specifies the geometry, the EMF exposures represented by Electro-Magnetic plane wave excitation, and the desired output parameters. The EMF exposure is determined by the external electric and/or magnetic fields for each scenario as determined by the EMF WORKSTATION calculations (EPRI). The calculation for the external electric field and magnetic field exposures are done separately. After the simulation is complete, we obtain the current density averaged over a square centimeter. Since the data generated by EMPIRE is not organ or tissue specific, MATLAB programs were developed for data post-processing. In the post-processing stage we vectorially add the induced average current density (ACD) from exposure to the external electric and magnetic

Table 3. The maximum values of the external electric and magnetic field exposures for the six scenarios.

Scenario #	Magnetic Flux Density B (mT)	Electric Field E (kV/m)
1	0.0521	4.949
2	0.062151	6.065
3	0.0664	6.485
4	0.00214	0.165
5	0.003729	0.745
6	0.00914	1.689

fields to determine the resultant ACD for each voxel. We determine the induced electric field for each voxel by dividing the ACD by the tissue conductivity at 60 Hz. We determine the maximum and average current densities and electric fields for any desired tissue or organ. The maximum and average current density for any cross section of the body in the x, y, or z direction can also be obtained.

3. RESULTS

3.1. External Field Exposures

EMF WORKSTATION simulations were performed for each scenario at different heights (0.50, 0.75, 1.00, 1.25, 1.50 and 1.75 m). The height of 1.75 m corresponds to about the middle of the head of the VH. To simulate the worst case scenario, the maximum value of both the electric and magnetic fields were selected for the computation of the internal electric field and current densities induced inside the human body using the EMPIRE software.

Table 3 shows the maximum values of the external electric and magnetic field exposures for the six scenarios. All the electric field values are below the IEEE controlled environment limit of 20 kV/m. The magnetic field values are also below the IEEE external magnetic field limits of 2.71 mT for the head and torso for controlled environment. The electric and magnetic field values are also lower than the limits specified by the ICNIRP, NRPB and ACGIH. The highest exposure level for both B (663.58 mG) and E (6.485 kV/m) is at scenario No. 4, which corresponds to a worker standing in the bucket close to conductor phase C and about 2 m away from the conductor; the minimum exposure level for both B (21.38 mG) and E (0.165 kV/m) is at scenario No. 5, which corresponds to a worker standing on the ground and at the edge of the right-of-way of the transmission line.

## 3.2. Induced Electric Field and ACD in Body Organs and Tissues

3.2.1. Scenario 3

In this scenario, a worker is standing in the bucket at 2 m away from phase C conductor. The external electric field is from front to back (**Ey = 6.485 kV/m**). The external magnetic field is from head to feet (**Bz = 664 mG**). The human body is in free space and not in contact with electrical ground. This is the scenario that has the highest electric and magnetic field values and hence is the worst case scenario in this study.

Table 4 shows the induced average current density, maximum current density, induced average electric field and induced maximum electric field for selected body organs. The values for all the voxels in each organ are used to calculate the maximum and average values of the current density and electric field. The calculated values for the hands and feet include all the tissues in these body parts except the skin. The values for the induced electric fields are obtained by dividing

Table 4. Scenario 3: Organ averaged current density $\mathbf{J}_{\text{avg}}$, maximum current density $\mathbf{J}_{\text{max}}$, averaged electric field $\mathbf{E}_{\text{avg}}$, and maximum induced electric field $\mathbf{E}_{\text{max}}$ for selected tissues. ($Ey = 6.485 \,\text{kV/m}$, $Bz = 664 \,\text{mG}$).

Tissue Type	$\mathbf{J}_{\text{avg}}$ (mA/m^2)	$\mathbf{J}_{\text{max}}$ (mA/m^2)	$\mathbf{E}_{\text{avg}}$ (mV/m)	$\mathbf{E}_{\text{max}}$ (mV/m)
Cerebellum	0.18	0.90	1.83	8.99
Gray Matter	0.33	1.49	4.10	18.59
White Matter	0.23	1.26	4.23	22.93
Heart	0.33	1.11	3.77	12.88
Nerve (Spine)	0.25	1.06	8.95	38.47
Eye (Aqueous Humor)	0.50	0.69	0.33	0.46
Kidneys	0.13	0.38	1.39	4.07
Liver	0.14	1.83	3.72	49.39
Lung (Inner)	0.18	1.81	2.64	25.83
Lung (Outer)	0.38	1.62	1.85	7.88
Pancreas	0.29	0.64	0.55	1.23
Spleen	0.18	1.18	2.00	13.18
Feet and Ankles	0.37	1.89	450.86	1111.95
Hands and Wrist	0.58	2.68	24.53	1041.19

(a) Layer Average Current Density
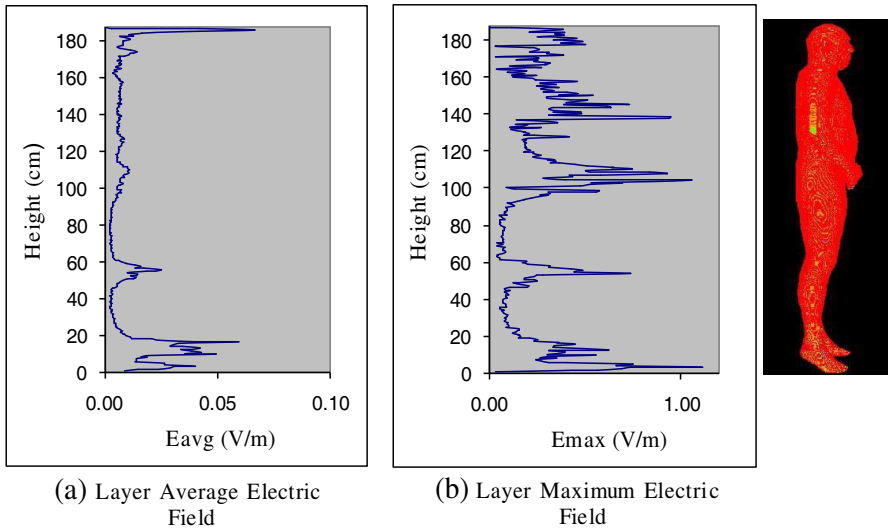
(b) Layer Maximum Current Density
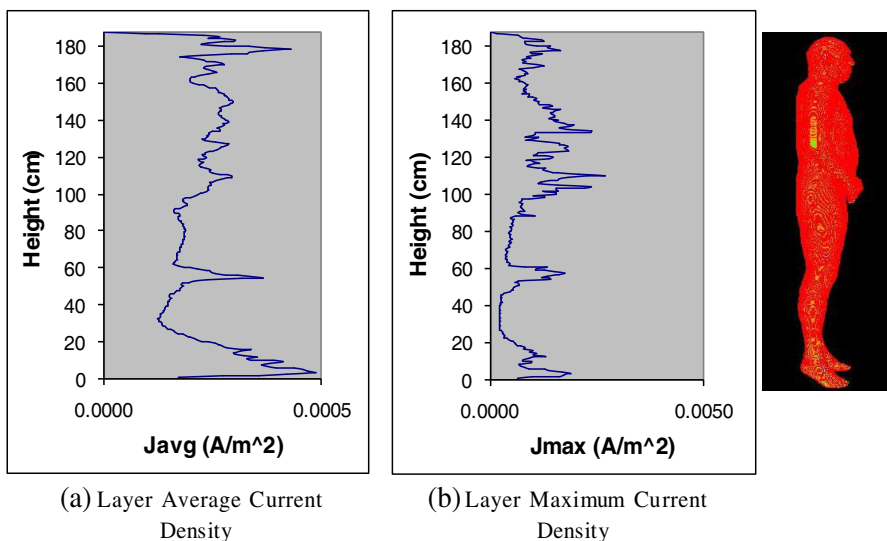
Figure 2. Scenario 3: (a) The layer-averaged current density J_{avg} and (b) the layer-maximum current density J_{max}. The layers are from the bottom of the feet (height $= 0$ cm) to top of the head (height $= 187$ cm).

the current density at each voxel by the conductivity of that voxel as specified by the human body model.

Figures 2 and 3 show the average and maximum current densities and the average and maximum electric fields for body layers along the height of the standing human, excluding the skin and mucous membrane. We have excluded the values for the skin and mucous membrane because it is at the boundary between air and the human body tissues. At this boundary, the very high gradient of the induced electric field produces large errors in the linearization of the Maxwell's differential equations. Each average value of the electric field and the current density is the average for all the voxels in the corresponding cross-section (layer) of the body. The maximum values for the induced electric field are significantly higher than the average values. The large difference is due the large variation between the conductivities of body tissues. In general, the average and maximum current densities and electric fields reach the highest values in the parts of the body that have the smallest cross sectional area such as the hand and feet, fingers and toes.

Our results permit us to get each organ or tissue maximum Electric field and current density. For instance, Figures 4(a) show the location

(a) Layer Average Electric
Field

(b) Layer Maximum Electric
Field

Figure 3. Scenario 3: (a) The layer-averaged electric field E_{avg} and (b) The layer-maximum electric field E_{max}. The layers are from the bottom of the feet (height $= 0\,\mathrm{cm}$) to top of the head (height $= 187\,\mathrm{cm}$).

(a) Current Density in the Heart (A/m²)   (b) Anatomical section at 1398 mm height
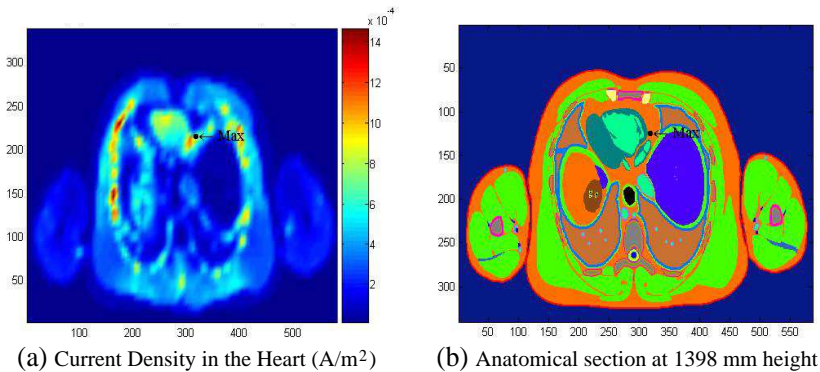
Figure 4. Scenario 3: (a) The location of maximum induced current density in the heart; (b) Anatomical cross section showing the location at which this maximal value occurs.

of maximum induced current density in the heart. The red color indicates the highest current densities and the blue color indicates the lowest values. Figures 4(b) show the anatomical structure of heart at which the maximum occur. Usually, the maximum values occur at

the boundaries between different tissues. This is shown by the arrow pointing at the boundary of the heart muscle. At the boundaries of different tissues, there are sudden changes of electrical tissue properties and hence higher voltage gradients, consequently higher electric fields and current densities.

3.2.2. Compliance with the Basic Restrictions for Internal Values

We compared the induced maximum current densities and electric fields to the maximum exposure limits listed in Table 2. Figure 5 shows the maximum induced currents for all scenarios for the brain, heart, hands, wrist, feet ankles and all other tissues. All the currents densities are below the NRPB [3] limit of $10\,\text{mA/m}^2$. It is interesting to note that scenario number 6 in which the worker is standing under the mid-span at a distance of about $10\,\text{m}$ from the cable gives overall the highest values of induced electric fields and current densities even when compared to scenario number 3 that has the highest external electric and magnetic fields. The difference is due to the fact that for scenario 6, the direction of the external electric and magnetic fields are from head to feet $(\mathbf{E}_z = \mathbf{1.689\,kV/m})$ and from front to back $(\mathbf{B}_y = \mathbf{91.41\,mG})$, respectively, while for scenario number 3 the external electric and magnetic fields are from front to back $(\mathbf{E}_y = \mathbf{6.485\,kV/m}$
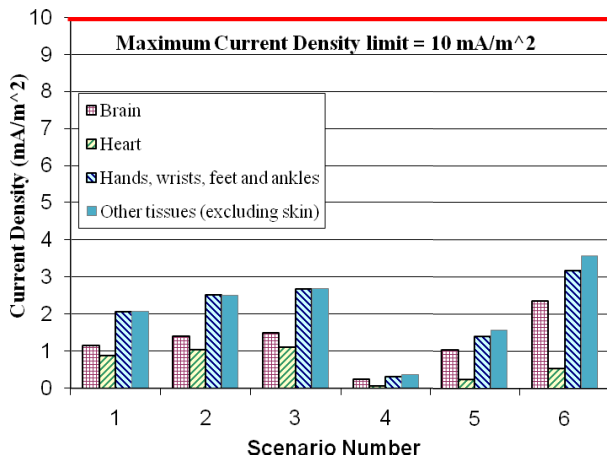
Figure 5. The maximum induced currents for all scenarios for the brain, heart, hands, wrist, feet ankles and all other tissues. All the currents densities are below the IEEE and the NRPB limit of $10\,\text{mA/m}^2$.

Table 5. The maximum induced electric field for all scenarios.

Exposure Tissue	IEEE Limit Emax (mV/m)	Scenario 1	Scenario 2	Scenario 3	Scenario 4	Scenario 5	Scenario 6
Brain	53.1	17.7	21.5	22.9	3.0	13.0	29.5
Heart	943	10.1	12.0	12.9	0.8	2.7	6.3
Hands, wrists, feet and ankles	2100	847.0	1037.0	1112.0	171.4	760.9	1726.4
Other tissues (excluding skin)	2100	103.3	125.6	134.2	17.1	72.7	165.4

and from head to feet $(\mathbf{B}_z = \mathbf{664\,mG})$ respectively. The former configuration gives better coupling with the human body and hence higher induced current densities and electric fields.

Table 5 shows the maximum induced electric field for all scenarios. All the induced electric fields are below the IEEE limit for workers. However, four out of six scenarios had exceeded the new 2010 ICNIRP limit of 800 mV/m [2]. In almost all scenarios, the maximum current densities and electric fields are observed in the bone marrow of the ankle and the knees. The higher current density in these sections is due to the fact that the body cross sectional area is small in these sections compared to the rest of the body.

4. CONCLUSION

We have simulated 6 different scenarios for a live line worker of a double circuit 132 kV transmission line. The electric and magnetic field values were found to be lower than the limits specified by the IEEE, ICNIRP, NRPB and ACGIH. The highest external electric field was 6485 V/m and the highest external magnetic field is 66.4 μT were found to be in scenario number 3 in which the worker is standing 2 meters away from phase C conductor. In all scenarios, the induced electric fields are below the IEEE occupational limit of 2100 mV/m. However, four out of six scenarios had exceeded the new 2010 ICNIRP occupational limit of 800 mV/m. The induced maximum current density in all the tissues was found to be below the NRPB limit of 10 mA/m². The highest values for induced electric fields and current densities for all the tissues except the heart was obtained for scenario number 6, in which the worker is standing under the mid-span at a distance of about 10 m from the nearest conductor. For the heart, the highest value of induced electric field and current density was obtained for scenario number 3. In general the highest values for each organ are obtained at

the border between different tissues. For the whole body the highest induced current densities occur in the body parts that have the lowest cross sections such as the hands feet and knees.

ACKNOWLEDGMENT

REFERENCES

1. *IEEE Standard for Safety Levels with Respect to Human Exposure to Electromagnetic Fields, 0–3 kHz.* IEEE Std C95.6, 2002.

2. ICNIRP, "Guidelines for limiting exposure to time-varying electric and magnetic fields (1 Hz to 100 kHz)," *Health Physics*, Vol. 99, No. 6, 818–836, 2010.

3. National Radiological Protection Board (NRPB), "Advice on limiting exposure to electromagnetic fields (0–300 GHz)," Vol. 15, No. 2, 2004, http://www.hpa.org.uk/Publications/Radiation/NPRBArchive/DocumentsOfTheNRPB/Absd1502/.

4. Gandhi, O. P. and J. Y. Chen, "Numerical dosimetry at power line frequencies using anatomically based models," *Bioelectromagn. J. Supp.*, Vol. 1, 43–60, 1992.

5. Dawson, T. W., J. DeMoerloose, and M. A. Stuchly, "Comparison of magnetically induced ELF fields in humans computed by FDTD and scalar potential FD codes," *Appl. Comput. Electromag. Soc. (ACES)*, Vol. 11, 63–71, 1996.

6. Zubal, I. G., C. R. Harrell, E. O. Smith, Z. Rattner, G. R. Gindi, and P. H. Hoffer, "Computerized three-dimensional segmented human anatomy," *Med. Phys. Biol.*, Vol. 21, 299–302, 1994.

7. Dimbylow, P. J., "FDTD calculations of the whole-body averaged SAR in an anatomically realistic voxel model of the human body from 1 MHz to 1 GHz," *Phys. Med. Biol.*, Vol. 42, 479–490, 1997.

8. Dimbylow, P. J., "Fine resolution calculations of SAR in the human body for frequencies up to 3 GHz," *Phys. Med. Biol.*, Vol. 47, 2835–46, 2002.

9. Gandhi, O. P., Y. G. Gu, J. Y. Chen, and H. I. Bassen, "Specific absorption rates and induced current distributions in an anatomically based human model for plane-wave exposures," *Health Phys.*, Vol. 63, 281–90, 1992.

10. Kuhn, S., W. Jennings, A. Christ, and N. Kuster, "Assessment of induced radio-frequency electromagnetic fields in various anatomical human body models," *Phys. Med. Biol.*, Vol. 54, 875–89, 2009.

11. Hand, J. W., "Modeling the interaction of electromagnetic fields (10 MHz–10 GHz) with the human body: Methods and applications," *Phys. Med. Biol.*, Vol. 53, R243–R286, 2008.

12. Dawson, T. W. and M. A. Stuchly, "High-resolution organ dosimetry for human exposure to low-frequency magnetic fields," *IEEE Trans. Mag.*, Vol. 34, No. 3, 708–718, 1998.

13. Furse, C. M. and O. P. Gandhi, "Calculation of electric fields and currents induced in a millimeter resolution human model at 60 Hz using the FDTD method," *Bioelectromagnetics*, Vol. 19, 293–299, 1998.

14. Gandhi, O. P., "Some numerical methods for dosimetry: Extremely low frequencies to microwave frequencies," *Radio Science*, Vol. 30, 161–177, 1995.

15. Gandhi, O. P., G. Kang, D. Wu, and G. Lazzi, "Currents induced in anatomic models of the human for uniform and nonuniform power frequency magnetic fields," *Bioelectromagnetics*, Vol. 22, 112–121, 2001.

16. Dimblylow, P. J., "Induced current densities from low-frequency magnetic fields in a 2 mm resolution, anatomically realistic model of the body," *Phys. Med. Biol.,* Vol. 43, 221–230, 1998.

17. Shen, L. and J. Kong, *Applied Electromagnetics*, Brooks/Cole Engineering Division, 1983.

18. Zahn, M., *Electromagnetic Field Theory: A Problem Solving Approach*, J. Wiley, 1979.

19. Rims, K. J. and P. L. Lawrenson, *Analysis and Computation of Electric and Magnetic Field Problems*, Pergamon Press, 1973.

20. Silvaster, P. and P. Ferrari, *Finite Element for Electrical Engineers*, Cambridge University Press, 1983.

21. Foe, P. Y. and S. Y. King, *Proc. IEE Bundle Conductors Electric Field by Integral Equations Method*, Vol. 123, No. 7, 702–706, 1976.

22. Maruvade, P. S. and W. Janischweskyj, *IEEE Trans. PAS Electrostatic Field of System of Parallel Cylindrical Conductors*, Vol. 88, No. 7, 1069–1078, 1969.

23. Singer, H., H. Steinbigler, and P. Weiss, "A charge simulation method for the calculation of high voltage fields," *IEEE Trans. PAS*, Vol. 93, 1660–1668, 1974.

24. El-Arabaty, A., M. Abdel-Salam, and E. Mansour, "Electric field

and corona threshold levels on HV biopolar transmission lines-calculations vs. experiment," *IEEE Trans. PAS*, Vol. 77, 236-3, 1977.

25. Sendaula, H. M., "Electric field induced by EHV transmission over irregular terrain," *IEEE Trans. PAS*, Vol. 102, No. 5, 1452–1458, 1983.

26. ERRI, *Transmission Line Reference Book 345 kV and Above*, Fred Weidner and Sons, New York, NY, 1975.

27. Electric Power Research Institute (EPRI), *Electric and Magnetic Fields Workstation (EMF WORKSTATION)*, Users Manual Version 2.5, 2007.

28. Deno, D. W. and L. E. Zaffanella, "Electrostatic effects of overhead transmission lines and stations," *Transmission Line Reference Book: 345 kV and Above*, 248–280, EPRI Report RP-68, Electric Power Research Institute, Palo Alto, Calif, 1975.

29. Yee, K. S., "Numerical solution of initial boundary value problems involving Maxwell's equations in isotropic media," *IEEE Tran. Antennas Propagation*, Vol. 14, 302–307, 1966.

30. Gandhi, O. P. and J. Y. Chen, "Numerical dosimetry at power-line frequencies using anatomically based models," *Bielectromagnetics J. Supplement*, Vol. 1, 43–60, 1992.

31. The U.S. National Library of Medicine, The Visible Human Project, http://www.nlm.nih.gov/research/visible/visible_human.html.

32. Maalej, N. M., T. K. Abdel-Galil, M. A. Abdul-Majeed, and I. O. Habiballah, *Organ Dosimetry for a Worker Standing Under a 132 kV Power Line*, World Congress on Medical Physics and Biomedical Engineering, Vol. 14, 2660–2663, 2007.

33. Maalej, N. M., C. A. Belhadj, T. K. Abdel-Galil, and I. O. Habiballah, "Visible human utilization to render induced electric field and current density images inside the human," *IEEE Proceedings*, Vol. 97, No. 12, 2053–2059, 2009.

34. Dawson, T. W., K. Caputa, and M. A. Stuchly, "Influence of human model resolution of computed currents induced in organs by 60 Hz magnetic fields," *Bioelectromagnetics*, Vol. 18, 478–490, 1997.

35. Gabriel, S. R., W. Lau, and C. Gabriel, "The dielectric properties of biological tissues: Measurements in the frequency range 10 Hz–20 GHz," *Phys. Med. Biol.,* Vol. 41, 2251–2269, 1996.